

# Design of a Grounded Low-Cost Capacitive Liquid Level Sensor for Robotics Applications, especially in the Field of Gastronomy

Nikolai Hangst, Steffen Schröder, Thomas M. Wendt, Lukas Stiglmeier, Philipp Gawron, and Urban B. Himmelsbach, Offenburg University of Applied Sciences, Work-Life Robotics Institute, 77652 Offenburg, Germany

## Abstract

This paper presents the development of a capacitive level sensor for robotics applications, which is designed for measurements of liquid levels during a pouring process. The proposed sensor design applies the advantages of guard electrodes in combination with passive shielding to increase resistance against external influences. This is important for reliable operations in rapidly changing measurement environments, as they occur in the field of robotics. The non-contact type sensor for liquid level measurement is the solution for avoiding contaminations and suit food guidelines. The designed sensor can be utilized in gastronomic applications. Two versions of the sensor were simulated, fabricated, and compared. The first version is based on copper electrodes, and the other type is fully 3D printed with electrodes made of conductive polylactic acid (PLA).

## 1 Introduction

In industry and society, the degree of automation is rising in all sectors. Robotics has become more advanced in recent years as well. Industrial and collaborative robots are applied in various applications [1, 2]. These robots can additionally be utilized as bartenders to prepare soft drinks, juices, cocktails, and serving beers. In this context, monitoring the liquid level in the cup is crucial for consistent product quality [3].

Existing sensors for continuous level measurement are applied in different fields. In general, different principles of measurement such as radar, ultrasonic, optical, or capacitive level sensing are suitable for continuous level measurement. Most of these sensors are specifically designed for applications in process tanks, containers, or silos. In robotics, especially for utilization in grippers, the usability of level sensors is restricted. Optical, ultrasonic, and radar sensors have limitations. They are dependent on transparent containers or must be placed near the edges, which reduces the application possibilities. In addition, they are complex and expensive in the associated electronic circuit. The presented sensor is based on a capacitive principle, allowing non-contact liquid level monitoring with a wide range of application options. Capacitive sensing has been accepted for its low cost, low power consumption and simple integration in different concepts [4]. Furthermore, the manufacturing of this sensor using 3D printing technology enables cost-efficient and flexible implementation of the sensor [5]. The non-contact design prevents contamination and qualifies the sensor for application in the food industry.

## 2 Design

The sensor design is based on a grounded parallel plate capacitor. This is attributed to a better capacitance change compared to the fringing field design determined in initial simulations. The sensor is based on sensing, shielding, two guard electrodes, and a ground electrode. The ground elec-

trode is located on the opposite side of the sensing electrode and forms the parallel plate capacitor. The sensor design is shown in Fig. 1.

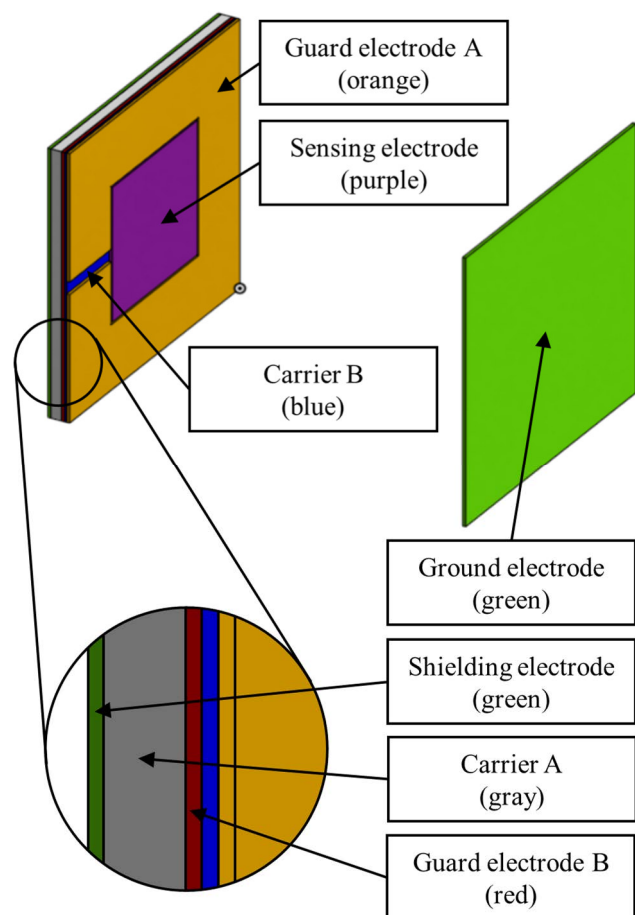


**Figure 1** Sensor design

The dimension of the sensor, which consists of all components mentioned in Fig. 1, is 60 mm x 60 mm x 4.4 mm (w x l x t). The ground electrode on the opposite has the same dimensions except for the thickness, which equals 0.6 mm. The distance between the electrodes is 80 mm.

This means a typical drinking cup fits between the electrodes. The sensing electrode measure 30 mm x 30 mm x 0.6 mm (w x l x t).

For the application of the sensor in the field of robotics, shielding against external influences is essential. For this purpose, the grounded shielding electrode with a thickness of 0.6 mm on the outside is necessary. Two different carrier parts keep the electrodes in position and isolate them from each other. The thickness of carrier B is 0.4 mm, carrier A 2.2 mm. This is related to the different function of both components. Carrier A serves as the primary carrier and provides stability. It also serves as a separating layer between the shielding and guarding electrode B. Carrier B isolates the sensing and guarding electrode B. Therefore, a thickness of 0.4 mm is sufficient.

The guard electrode A is arranged in a U-shape around the sensing electrode. Due to this design, the electric field of the measuring electrodes is directed in the measuring range, and the edge effects have a minor influence on the measured value. This provides linearity, precision, and accuracy [7–9]. A wire can be connected to the sensing electrode via the 2.8 mm notch. The guard electrodes A and B are designed for simplified fabrication. The layer-by-layer structure is advantageous with regard to manufacturing with a 3D printer.

### 3 Materials and Methods

#### 3.1 Materials and Machine

The developed sensor versions were manufactured with the Neotech AMT 15X SA with a 0.2 mm layer height and 100% filling density. One of the two versions was assembled from separately manufactured parts. The other one is fully 3D printed. The material utilized for the assembled capacitor is polylactic acid (Prusament PLA, Prusa Research) for the carrier parts and copper plates for the electrodes. The same non-conductive PLA is applied for the 3D printed version but with layers of conductive PLA from Proto-pasta. The conductive layers create the electrodes. No additional ink or other parts are needed. Copper wires are only required to integrate the electrodes into the evaluation circuit.

#### 3.2 Working Principle

A parallel plate capacitor is defined by connecting different potentials on two electrodes. In this case, the electric field will be generated between the positive and negative electrodes. The ideal capacitance  $C$  can be calculated with the following formula (1) [6]:

$$C = \epsilon_0 \epsilon_r \frac{A}{d} \quad (1)$$

$\epsilon_0$  is the permittivity of vacuum space,  $\epsilon_r$  is the permittivity of the dielectric material,  $d$  is the distance between the electrodes, and  $A$  is the area of the sensing plate. According to formula (1), the geometry from the electrodes and the

distance from the plates as well as material dielectric properties affect the capacitance of a parallel plate capacitor. The change in dielectric properties is crucial for level measurement [5].

#### 3.3 Modeling

There are different materials in the area between the plates. Therefore, formula (1) is invalid and has to be modified.

**Fig. 2** shows the equivalent circuit for the calculation of the ideal capacitance between the sensing electrode and ground.

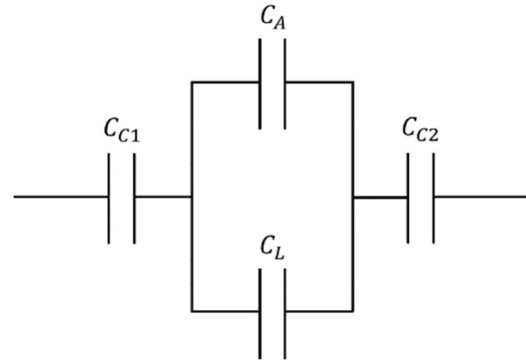


**Figure 2** Equivalent circuit for the sensing capacitance between the sensing electrode and ground

The inside of the cup can be considered as two parallel capacitors. The current liquid level separates the entire capacitor into a capacitor with air and a capacitor with liquid ( $C_A$  and  $C_L$ ). In addition, the cup walls must be regarded as capacitors connected in series ( $C_{C1}$  and  $C_{C2}$ ). According to this, the ideal capacitance of the sensor can be calculated by formula (2).

$$C = \frac{1}{\frac{1}{C_{C1}} + \frac{1}{C_A + C_L} + \frac{1}{C_{C2}}} \quad (2)$$

#### 3.4 Simulation

COMSOL Multiphysics was used for the finite element method (FEM). The simulation was performed with water as the filling medium with an  $\epsilon_r$  of 80.3. For the cup, an  $\epsilon_r$  of 3.6 was applied. The simulation of the electric field of the sensor with a liquid level of 30 mm water is shown in **Fig. 3**.

Region 1 and 3 represent the electric field of the guard electrode A and region 2 the field of the sensing electrode. As seen, the liquid has a strong influence on the electric field and the difference between the air section and the water section is visible. A directed field can be seen between the sensing electrode and ground. The red arrows pointing to the left show the effect of shielding. As a result of the second guard electrode B, the capacitance of the sensing electrode is not reduced by the shielding electrode.

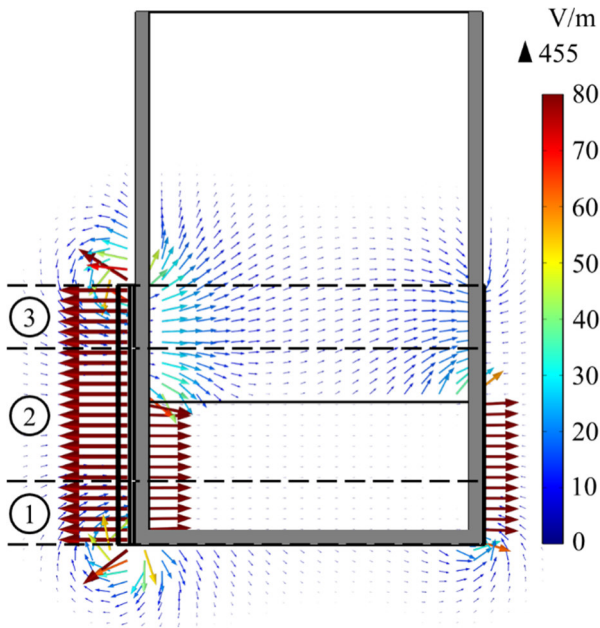


**Figure 3** Simulation of the electric field of the sensor with a liquid level of 30 mm water

### 3.5 Fabrication

**Fig. 4** shows the two versions of the manufactured sensor. The left one is made of copper plate electrodes and 3D printed carrier parts. The right one is fully 3D printed. This version is printed in one piece, eliminating the assembly process except for attaching the connecting wires. The copper electrodes from the left version are made of 0.6 mm copperplates.

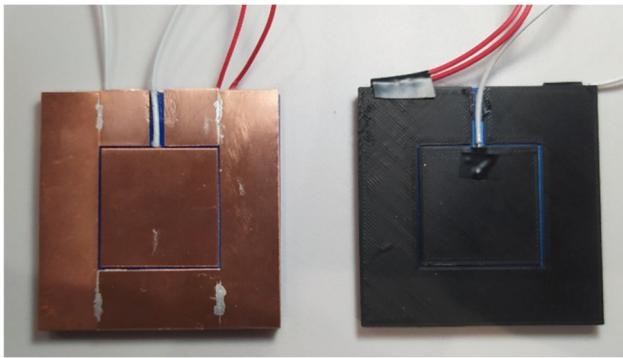


**Figure 4** The copper (left) and the 3D printed (right) version of the sensor

### 3.6 Experimental Setup

To verify the results of the simulations, the sensor design was evaluated in an experimental setup. For this purpose, the sensors were connected to a capacitance-to-digital converter (CDC). The EVAL-AD7747 board was applied to measure the capacitance. This board utilizes the AD7747 CDC to measure the capacitance with high accuracy ( $\pm 10$  fF) and linearity ( $\pm 0.01\%$ ). The CDC has a port for active shielding connected to the guard electrodes [10]. The Evaluation board was connected to a PC, on which the data is collected. The data has been evaluated in MATLAB. The schematic setup is shown in **Fig. 5**.

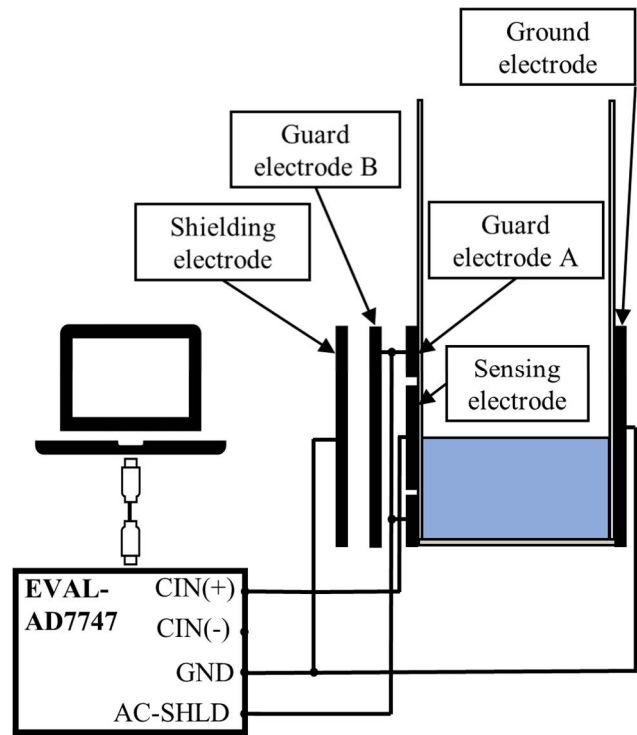


**Figure 5** Schematic experimental setup

For the measurements, a liquid is filled into a cup step by step, and 100 measurements for a statistically significant result are taken for the capacitance. This procedure is carried out with three different liquids: water, cola, and beer.

## 4 Results

### 4.1 Verification of the Simulated Values

The simulated capacitance was compared through an experiment with water. The selection of water is based on the known dielectric properties.

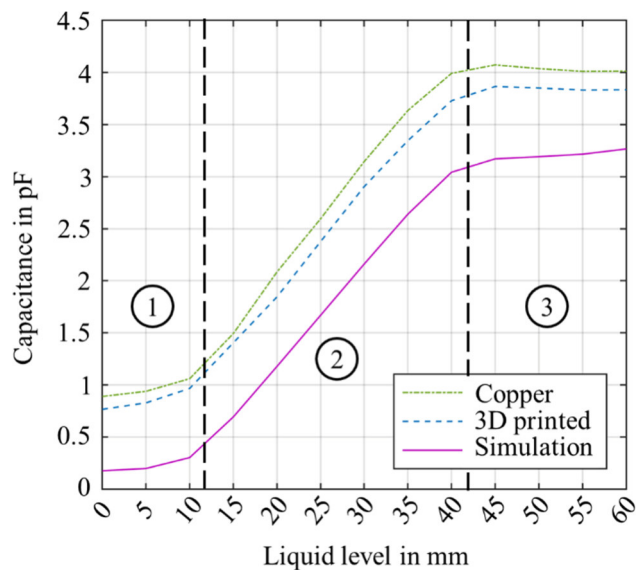


**Figure 6** Simulated and measured capacitance of the sensors with water as filling liquid

Fig. 6 shows the capacitance related to the liquid level. Region 2 represents the sensing field. Region 1 and 3 show the effect of the residual fringing field at the sensor electrode. As a result of the alignment of the entire sensor in the lower area of the cup, the operating range of the sensing electrode starts at 12 mm and extends to 42 mm (Fig. 3, and Fig. 5).

The average standard deviation (SD) of the measured values for both versions is shown in Tab. 1. The SD increases with foaming liquids (cola and beer).

**Table 1** Average SD of the measured values for the two sensor versions

| Liquid | SD copper               | SD 3D printed           |
|--------|-------------------------|-------------------------|
| Water  | $1.85 \cdot 10^{-4}$ pF | $3.12 \cdot 10^{-4}$ pF |
| Cola   | $6.28 \cdot 10^{-4}$ pF | $5.23 \cdot 10^{-4}$ pF |
| Beer   | $11.1 \cdot 10^{-4}$ pF | $6.45 \cdot 10^{-4}$ pF |

## 4.2 Characteristic Behavior of the Copper Version

The values of the measured capacitance for the copper version with different liquids are shown in Fig. 7. Regions 1, 2 and 3 show the different areas in the same way as in chapter 4.1. The characteristic behavior of the sensor is similar for different liquids except for beer.

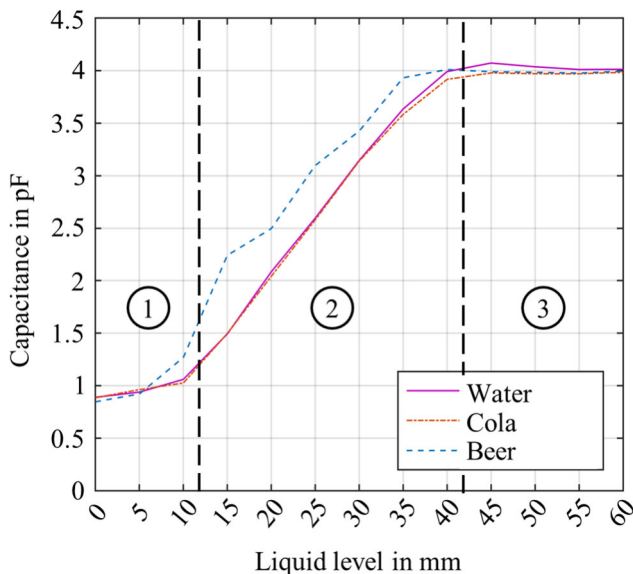


**Figure 7** Measured capacitance of the copper version with different liquids at different liquid levels

## 4.3 Characteristic Behavior of the 3D Printed version

The results of the 3D-printed version are shown in Fig. 8. The characteristic behavior of this sensor with different liquids is similar to the copper version. A deviation can equally be seen for beer. The division into three regions as described in chapter 4.1 is replicated.

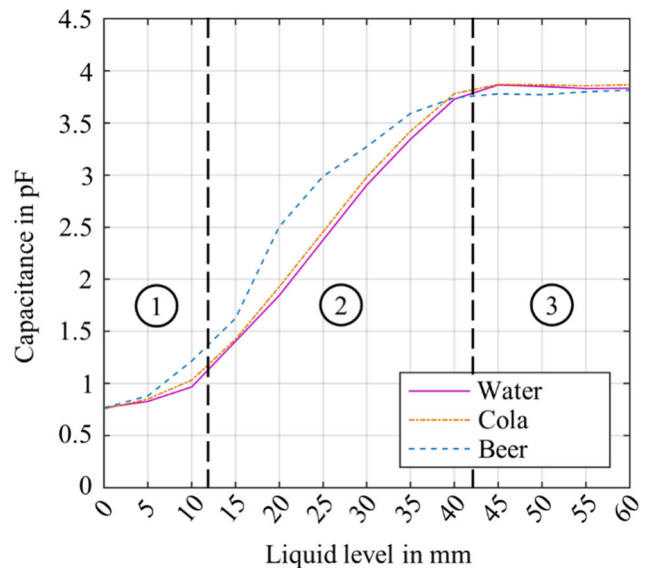


**Figure 8** Measured capacitance of the 3D printed version with different liquids at different liquid levels

## 5 Discussion

Fig. 6 shows an offset between the simulated and measured values of the sensor. This is related to the parasitic capacitance of the connecting wires, which were not considered in the simulation. The offset was compensated for the comparison with the measured values.

Compared to the simulation, the average deviation of the measured capacitance change between a fill height from 0 mm to 60 mm is 0.033 pF or 1.08% for the copper version. The deviation for the 3D printed version is -0.022 pF or -0.71%. The 3D printed version is closer to the Simulation than the copper version. This is a result of more precise manufacturing of the 3D printed type. Generally, the simulated values are confirmed by the measurement performed on both versions.

The sensor shows an approximately linear behavior in both versions except for foaming beer (Fig. 6, Fig. 7, and Fig. 8). The capacitance fluctuations at the edges of the sensing electrode as a result of fringing field effects could be minimized by applying guard electrodes.

The non-linearity of the beer curves for both versions (Fig. 7, and 8) is attributable to the inaccuracy filling process and the resulting foaming. This also explains the higher SD than the other liquids (Tab. 1). Cola is also foaming, which is shown by a larger SD compared to water. However, this foaming is significantly lower compared to beer.

## 6 Conclusion and Outlook

An effective capacitive non-contact level sensor for different liquids was modeled, simulated, fabricated, and evaluated. The sensor was fabricated in two versions, an assembled sensor made of copper plates and a fully 3D printed version. The experimental results verify the simulation and the functionality of both. Mediums such as foam can be

detected with the sensor as well. This effect can be applied to prevent foaming over the edge of cups.

The successful manufacturing of the sensor with 3D printing creates new design possibilities and low-cost options. This enables a simple fabrication of complex components with integrated capacitive sensors or other sensor technologies. The sensors are scalable and customizable to new applications. Regarding Industry 4.0, the advantages of 3D printed sensors are crucial, too. The requirement for customized and cost-efficient sensor is continuously increasing.

## 7 Acknowledgement

Funded by the Deutsche Forschungsgemeinschaft (DFG, German Research Foundation) – 426605889

## 8 Literature

- [1] U. B. Himmelsbach, T. M. Wendt, N. Hangst, P. Gawron, and L. Stiglmeier, “Human-Machine Differentiation in Speed and Separation Monitoring for Improved Efficiency in Human-Robot Collaboration,” *Sensors* (Basel, Switzerland), vol. 21, no. 21, 2021, doi: 10.3390/s21217144.
- [2] R. D. Atkinson, „Robotics and the Future of Production and Work“. Information Technology & Innovation Foundation: 2019. Available online: <https://itif.org/publications/2019/10/15/robotics-and-future-production-and-work> (accessed: Mar. 13 2022).
- [3] M. Stopfkuchen, N. Hangst, and T. M. Wendt, “O’Barro - Cocktails 4.0,” in vol. 45, *Campus: Magazin der Hochschule Offenburg*, 2019, pp. 90–91.
- [4] C. S. S. Babu and P. Manohar, “Design of a low cost signal conditioning circuit for self-compensated non contact capacitive type multi threshold liquid level sensor,” in *International Conference on Circuits, Communication, Control and Computing*, Bangalore, India, Nov. 2014 - Nov. 2014, pp. 58–63.
- [5] S. J. Leigh, R. J. Bradley, C. P. Pursell, D. R. Billson, and D. A. Hutchins, “A simple, low-cost conductive composite material for 3D printing of electronic sensors,” *PloS one*, vol. 7, no. 11, e49365, 2012, doi: 10.1371/journal.pone.0049365.
- [6] W. c. Heerens, “Basic principles in designing highly reliable multi-terminal capacitor sensors and performance of some laboratory test models,” *Sensors and Actuators*, vol. 3, pp. 137–148, 1982, doi: 10.1016/0250-6874(82)80015-2.
- [7] M. C. Hegg and A. V. Mamishev, “Influence of variable plate separation on fringing electric fields in parallel-plate capacitors,” in *Conference Record of the 2004 IEEE International Symposium on Electrical Insulation*, Indianapolis, IN, USA, Sep. 2004, pp. 384–387.
- [8] J. Pusppanathan et al., “FINITE ELEMENT ANALYSIS ON ELECTRICAL CAPACITANCE SENSOR GUARD,” *Jurnal Teknologi*, vol. 77, no. 28, 2015, doi: 10.11113/jt.v77.6792.
- [9] X. B. Li, S. D. Larson, A. S. Zyuzin, and A. V. Mamishev, “Design principles for multichannel fringing electric field sensors,” *IEEE Sensors J.*, vol. 6, no. 2, pp. 434–440, 2006, doi: 0.1109/JSEN.2006.870161.